Cellular and Molecular Neurobiology (2019) 39:461–470
https://doi.org/10.1007/s10571-019-00662-y

ORIGINAL RESEARCH

The MicroRNA Expression Profiles of Human Temporal Lobe Epilepsy in HS ILAE Type 1

Chongyang Tang[1] · Haiyang Wang[1] · Hongmei Wu[2] · Shi Yan[1] · Zhibin Han[1] · Zhenfeng Jiang[1] · Meng Na[1] · Mian Guo[3] · Dunyue Lu[1] · Zhiguo Lin[1]

Received: 20 December 2018 / Accepted: 11 February 2019 / Published online: 21 February 2019

Abstract

Temporal lobe epilepsy (TLE) is associated with neurodegeneration, often leading to hippocampal sclerosis (HS). Type 1 HS, which is characterized by severe neuronal loss and gliosis predominantly in regions CA1 and CA4, is the most common subtype and is associated with the best prognosis according to the ILAE classification system. MiRNAs participate in the biological processes underlying many nervous system diseases, including epilepsy. However, the miRNA expression profile of HS ILAE type 1 is not completely understood. A total of 14 patients were identified as having the ILAE subtype, as determined by NeuN immunohistochemistry (ILAE type 1 = 7; no-HS = 7). Next-generation sequencing and reverse transcription polymerase chain reaction technology were used to validate the dysregulated miRNAs. Bioinformatics analysis of the predicted target genes was conducted using Gene Ontology and Kyoto Encyclopedia of Genes and Genomes analyses. In total, 1643 mature miRNAs were detected in this study, along with 5 miRNAs that were upregulated and 2 miRNAs that were downregulated in the type 1 group. Bioinformatics analysis showed that 1545 target genes were predicted using the miRDB and Targetscan databases and that these predicted genes showed enrichment in pathways associated with nucleic acid binding, intracellular and cellular macromolecule metabolic processes, and the PI3K-Akt signaling pathway. This study is the first to report the miRNA expression profile of HS ILAE type 1 compared with those of no-HS. These results provide new insights into the neuronal loss pathology of type 1 HS.

Keywords TLE · HS ILAE classification · MiRNA profiling · Target prediction · Next-generation sequencing

Abbreviations

AEDs	Antiepileptic drugs
BDNF	Brain-derived neurotrophic factor
EEG	Electroencephalogram
FDR	False discovery rate
GO	Gene Ontology
HS	Hippocampal sclerosis
ILAE	International League Against Epilepsy
KEGG	Kyoto Encyclopedia of Genes and Genomes
MRI	Magnetic resonance imaging
NGS	Next-generation sequencing
FDG-PET/CT	Fluorodeoxyglucose-positron emission tomography combined with computed tomography
PFA	Paraformaldehyde
ROS	Reactive oxygen species
RT-PCR	Reverse transcription polymerase chain reaction
TLE	Temporal lobe epilepsy
TPM	Transcripts per million
UTR	Untranslated region

Chongyang Tang and Haiyang Wang have contributed equally to this study.

Electronic supplementary material The online version of this article (https://doi.org/10.1007/s10571-019-00662-y) contains supplementary material, which is available to authorized users.

✉ Zhiguo Lin
zhiguolin@outlook.com

[1] Department of Neurosurgery, The First Affiliated Hospital, Harbin Medical University, Harbin, Heilongjiang 150001, People's Republic of China

[2] Department of Pathology, The Fourth Affiliated Hospital, Harbin Medical University, Harbin, People's Republic of China

[3] Department of Neurosurgery, the Second Affiliated Hospital, Harbin Medical University, Harbin, People's Republic of China

Introduction

Epilepsy is one of the most commonly occurring chronic disorders of the central nervous system, affecting more than 50 million individuals all over the world. It is characterized by recurrent unprovoked seizures due to cortical neuron abnormalities (Alsharafi et al. 2015). In epileptic patients, one-third of cases that did not demonstrate an adequate response to antiepileptic drugs (AEDs) were determined to have drug-resistant epilepsy. Temporal lobe epilepsy (TLE) is one of the most frequently occurring types of drug-resistant epilepsy found in clinical settings; it is the most common form of epilepsy in adult patients and requires resection of the epileptic zone for treatment (Wang et al. 2015). The most common histopathologic abnormality of TLE is hippocampal sclerosis (HS), and surgery of the epileptogenic zone includes resection of the hippocampus. In 2013, the International League Against Epilepsy (ILAE) proposed a classification system for TLE-HS, and three types were identified. HS ILAE type 1 is the most commonly observed HS type and is diagnosed in approximately 60–80% of all patients with TLE; it is defined by severe neuronal loss and gliosis that predominantly affects the CA1 and CA4 regions (Blümcke et al. 2013). Type 2 is predominantly characterized by neuronal loss and gliosis in CA1, while type 3 is marked by severe neuronal loss and gliosis in CA4. There is another type of TLE that affects the hippocampus, exhibits reactive gliosis only, and does not feature neuronal loss; this type is referred to as no-HS (Blümcke et al. 2013).

MicroRNA (miRNA) is a single-strand endogenous noncoding RNA that modulates posttranscriptional gene expression. The mature form of miRNA consists of 18–22 nucleotides and binds to the 3′ or 5′ untranslated region (UTR) of the target mRNA. MiRNAs participate in the regulation of numerous physiological processes, and dysregulated miRNAs play an important role in disease development. In all organs of the human body, the brain has the highest abundance of miRNAs, likely due its complex functions (Bagla et al. 2018). Evidence has provided insight into the changes in miRNA expression profiles in neurological diseases, such as gliomas (Dai et al. 2017), ischemia (Sørensen et al. 2014), and epilepsy (et al. 2012; McKiernan et al. 2012). Several studies on epilepsy showed that the miRNA expression profiles were altered in various animal models and human tissues; in particular, miRNAs were relevant to seizure-induced neuronal death or neuroprotection (Roncon et al. 2015; Surges et al. 2016). Conversely, dysregulation of miRNAs may benefit the diagnosis of TLE and therapeutic approaches used to manage it.

In our previous research (Na et al. 2015), we found that the most favorable seizure outcomes after surgery included identification of the HS ILAE type 1 group, and this result corresponded with the findings of the ILAE study. However, the molecular reasons underlying the different prognosis in TLE patients of the various ILAE subtypes remain to be elucidated. Researching the markers, including the miRNA profiles, associated with the various pathological manifestations could help to better understand the biological process of HS ILAE type 1. The goal of this study was to explore the changes in miRNA expression profiles between HS ILAE type 1 and no-HS type patients with TLE. For this research, we performed next-generation sequencing (NGS) of the hippocampus in three patients with ILAE type 1 and the no-HS type. Seven dysregulated miRNAs were discovered; in all of them, aberrant miRNAs were identified by quantitative real-time polymerase chain reaction (qRT-PCR) in 14 hippocampal tissue samples. Bioinformatics analysis was used to evaluate the function of their predicted targets. This study may provide information on the molecular basis underlying the pathogenesis of patients with type 1 TLE.

Methods

Patients

All 14 patients underwent anteromesial temporal resections at the First Affiliated Hospital of Harbin Medical University in China within the period 2014–2017. Drug-resistant epilepsy was defined according to the consensus proposed by the ILAE (Kwan et al. 2010). The diagnosis of TLE was made based on the ILAE criteria for all patients. The preoperative examination included 3.0T magnetic resonance imaging (MRI) of the hippocampus, electroencephalogram (EEG), video-electroencephalographic monitoring, cognitive and neuropsychological testing, and interictal fluorodeoxyglucose-positron emission tomography combined with computed tomography (FDG-PET/CT). Two independent physicians conducted the preoperative evaluations. All patients underwent selective amygdalohippocampectomies or standard anterior temporal lobectomies with amygdalohippocampectomies performed by the same surgeon (Surgeon Lin ZG). During the operation, cortical and depth electrode recordings were performed to further confirm the abnormal electrical activity. All subjects in this study provided their written informed consent. The study protocol was approved by the Ethics Committee of the First Clinical College of Harbin Medical University.

Tissue Preparation

Hippocampal specimens were dissected into 5-mm-thick slices along the anterior-posterior axis. One slice was fixed

with 4% paraformaldehyde (PFA) overnight and then dehydrated and embedded in paraffin. Other fresh tissue slices were stored in liquid nitrogen for future experiments. To control for population bias among the resected tissues, the body of the hippocampus was resected in each sample for next-generation sequencing and RT-PCR (Fig. S1).

Immunohistochemistry

A coronal section with a thickness of 4 μm was sliced from the paraffin-embedded hippocampal tissue. After being deparaffinized by xylene and gradient ethanol hydration, the hippocampal tissue sections were incubated in mouse anti-NeuN monoclonal antibody (Zhongshan Golden Bridge Biotechnology, Beijing, People's Republic of China). Then, the sections were stained with anti-mouse or anti-rabbit immunoglobulin and streptavidin-conjugated horseradish peroxidase. Finally, 3,3′-diaminobenzidine was added as a chromogen, and the sections were evaluated using light microscopy. The HS types in our samples were defined according to the international consensus classification of HS in TLE by the ILAE (Blümcke et al. 2013). Type 1 was identified as having severe neuronal loss and gliosis that predominantly affected the CA1 and CA4 regions, while the no-HS control group in this study demonstrated maintenance of a normal number of neurons with reactive gliosis but only in the hippocampal specimens. The quantitative measurement of neuronal cell number was performed as previously described (Na et al. 2015). The number of neurons was counted in 4 visual fields in CA4 and in 10 visual fields in CA1 at 200x objective magnification, representing 1.21 mm^2. The mean number of neurons/mm2 was calculated. Assessment of hippocampal subtypes and cell counts was evaluated by two independent neuropathologists in a blinded manner. The difference in neuronal cell number between the ILAE type 1 group and the no-HS group was evaluated with the Mann–Whitney test. A value of $p < 0.05$ was considered statistically significant.

RNA Isolation and Quality Control

Total RNA was extracted from the frozen hippocampal tissues using TRIzol Reagent (Thermo Fisher Scientific, Waltham, MA, USA), as previously described (Tang et al. 2018). RNA purity and concentration were assessed using a NanoPhotometer® spectrophotometer (Implen GmbH, Munich, Germany) and a Qubit® RNA Assay Kit with a Qubit® 2.0 Fluorometer (Thermo Fisher Scientific). An RNA Nano 6000 Assay Kit and a Bioanalyzer 2100 system (Agilent Technologies, Santa Clara, CA, USA) were used to measure RNA integrity.

Library Preparation and Sequencing

Next, 3 μg of total RNA per sample was used to prepare the small RNA library; the sequencing libraries were generated using a NEBNext® Multiplex Small RNA Library Prep Set for Illumina® (NEB, Ipswich, MA, USA.) following the manufacturer's recommendations. Then, the index codes were added to attribute sequences to each hippocampus sample. Finally, library quality was assessed on an Agilent Bioanalyzer 2100 system using DNA High Sensitivity Chips.

According to the manufacturer's instructions, the clustering of the index-coded hippocampus samples was performed on a cBot Cluster Generation System using a TruSeq SR Cluster Kit v3-cBot-HS (Illumina, San Diego, CA, USA). After cluster generation, the libraries were sequenced on an Illumina HiSeq 2500 platform, and 50 bp single-end reads were generated.

Sequence Data Analysis

To control for data quality, raw reads in the fastq format were first processed through custom Perl and Python scripts. The clean reads obtained in this step were mapped to the reference sequence using Bowtie (Langmead et al. 2009). Subsequently, for the mapped small RNA tags, miRBase20.0 was used as a reference; the modified software mirDeep2 (Friedländer et al. 2012) and sRNA-tools-cli were used to obtain the potential miRNA and draw the secondary structures. MiRNA expression levels were normalized via transcripts per million (TPM). The following normalization formula was used:

$$\text{Normalized expression} = \text{mapped readcount}/\text{Total reads} * 1000000$$

The DESeq R package was used to analyze differential expression between the ILAE type 1 group and the no-HS group. The original false discovery rate (FDR) method of Benjamini and Hochberg was used to adjust the p value. An adjusted p value of < 0.05 was considered statistically significant.

The predicted target gene for each miRNA was obtained from the miRDB and Targetscan databases. The target gene candidates of the differentially expressed miRNAs were used for Gene Ontology (GO) enrichment and Kyoto Encyclopedia of Genes and Genomes (KEGG) analysis. GO and KEGG analyses were performed with the online tool DAVID (http//david.abcc.ncifcrf.gov); adjusted p values < 0.05 were deemed significant.

miRNA Validation

MiRNA from 14 samples was reverse transcribed using a Transcriptor First Strand cDNA Synthesis kit (Hoffmann-La Roche, Basel, Switzerland). MicroRNA-specific primers (Ribobio Guangzhou, People's Republic of China) were used for reverse transcription of all miRNA candidates. RT-PCR was performed with SYBR Green Master Mix using an ABI7500 Fast Realtime system (Applied Biosystems, Foster City, CA, USA). The endogenous, small-nuclear RNA U6 was used for the normalization of all miRNAs. The real-time PCR cycling conditions were as follows: 95 °C for 10 min, 45 cycles at 95 °C for 15 s, and 60 °C for 60 s. The melt curve stage was set as follows: 95 °C for 15 s, 60 °C for 60 s, and 95 °C for 15 s. The relative fold change in the expression of miRNAs was determined using the 2-ΔΔCt method. The difference in miRNA expression between the ILAE type 1 group and the no-HS group was evaluated with the Mann–Whitney test by GraphPad Prism 7.0 software. A value of $p < 0.05$ was considered statistically significant.

Results

Clinical and Pathological Characteristics

The clinical data related to HS ILAE type 1 and the no-HS type are shown in Table 1. The average age of all patients was 24.7 years, ranging from 12 to 31 years. There were no significant differences between the ILAE type group and no-HS group in patient age ($p > 0.05$, Mann–Whitney test). The average age of the first seizure for all patients was 14.5 years, ranging from 4 to 29 years. There was a statistically significant difference in the age of the first seizure between these two groups ($p < 0.05$, Mann–Whitney test), and this finding was consistent with a previous study (Blümcke et al. 2007). All patients had been unable to control their seizures with more than two different antiepileptic drugs. Neuropathological examination, which consisted of NeuN immunostaining of the tissues from ILAE type 1 and no-HS type, was carried out in this study (Fig. 1). In all ILAE type 1 samples, the typical pathological characteristics of severe neuronal loss and gliosis in the CA1 and CA4 regions were observed for all cases (Fig. 1b). No-HS tissues did not show significant neuronal loss; they exhibited only reactive gliosis (Fig. 1a). A semiquantitative analysis was used to compare the difference in neuron density between the two groups. The neuronal loss in the CA1 and CA4 regions in the ILAE type 1 group was more severe than that in the No-HS group ($p < 0.001$, Fig. 1c).

MicroRNA Expression Profiling in ILAE Type 1 and Controls

High-throughput sequencing was performed to determine the miRNA expression between the ILAE type 1 group and the control group in this study. In assessing the quality of the RNA samples, the RIN values of all samples were above 7.5. Supplementary Table 1 provides the total sequence reads for all samples. We obtained 80.8 million sequence reads in both the control and ILAE type 1 groups. After filtering low-quality reads and screening the reads in the 18–35 nt

Table 1 Clinical data of HS ILAE type 1 and no-HS patients

Sample	Age at surgery (years)	Gender	Hippocampus	First seizure of age (years)	AEDs	ILAE classification	RNA-Seq
I1	24	M	L	9	PHB LEV VPA	ILAE-I	Y
I2	29	M	L	9	CBZ LTG	ILAE-I	Y
I3	29	F	L	4	VPA LEV TPM	ILAE-I	Y
I4	15	M	L	7	VPA OXC LTG LEV	ILAE-I	N
I5	21	F	R	18	CBZ VPA	ILAE-I	N
I6	12	F	R	8	OXC LEV LTG	ILAE-I	N
I7	27	F	L	13	PHB CBZ TPM	ILAE-I	N
C1	27	M	L	22	PHB VPA TPM	no-HS	Y
C2	31	M	R	29	OXC VPA LTG	no-HS	Y
C3	30	F	R	27	PHB LEV VPA	no-HS	Y
C4	19	M	R	9	PHB OXC	no-HS	N
C5	29	M	L	14	VPA OXC CBZ	no-HS	N
C6	24	F	R	14	CBZ OXC LEV	no-HS	N
C7	29	F	R	20	LEV VPA	no-HS	N

AEDs antiepileptic drugs, *CBZ* carbamazepine, *LEV* levetiracetam, *LTG* lamotrigine, *PHB* phenobarbital, *TPM* topiramate, *VPA* valproic acid, *OXC* oxcarbazepine

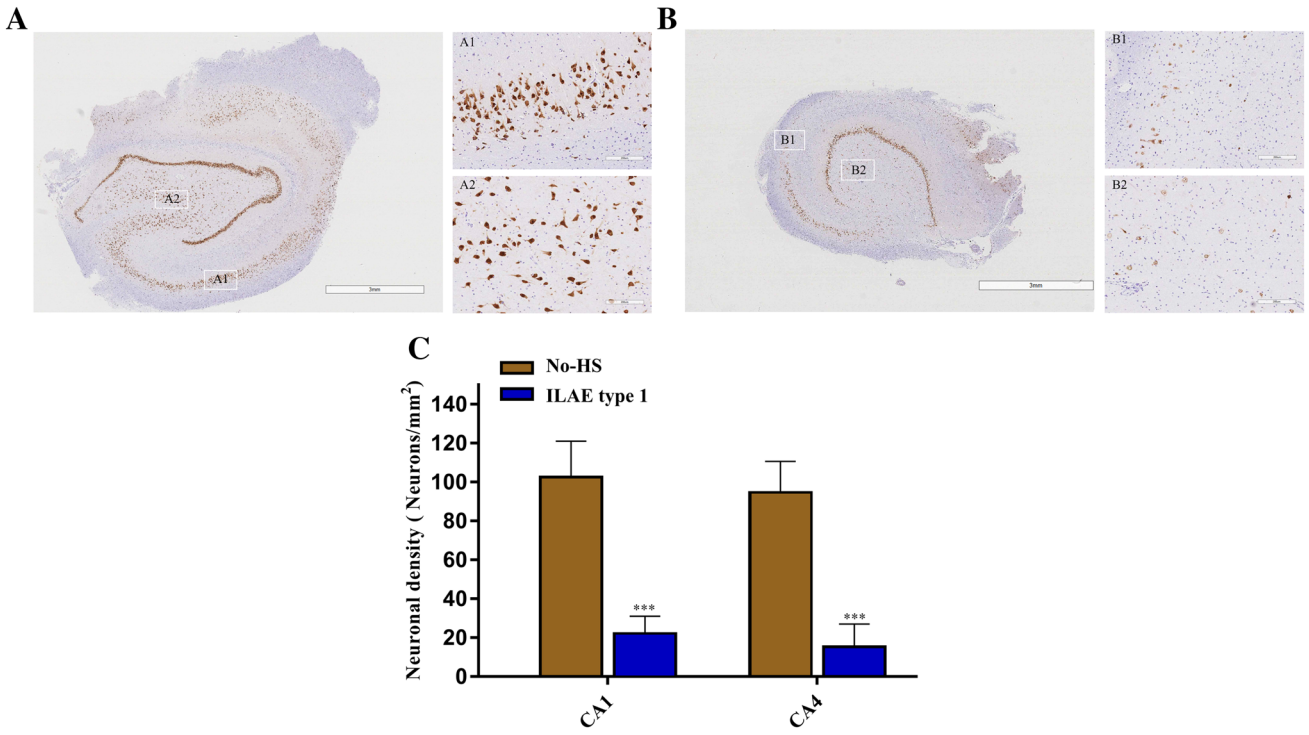

Fig. 1 Immunohistochemical NeuN staining of HS ILAE type 1 and no-HS type. **a** Low-magnification view of the no-HS type showing no features of neuronal loss in the CA1 and CA4 regions; (*A1*) High-magnification view of the no-HS type in CA1; (*A2*) High-magnification view of the no-HS type in CA4. **b** Low-magnification view of the HS ILAE type 1 showing features of neuronal loss in the CA1 and CA4 regions; (*B1*) High-magnification view of the HS ILAE type 1 in CA1; (*A2*) High-magnification view of the HS ILAE type 1 in CA4. Scale bars = 3 mm (**a, b**) and 200 μm (*A1, A2, B1, B2*). **c** Comparison of neuronal density between the HS ILAE type 1 and No-HS groups ($^{***}p < 0.001$)

scope, a total of 75.8 million reads were retained for further analysis (Table S2). The sequence length distribution from 18 to 35 nucleotides for each sample is shown in Supplementary Fig. 2. We aligned these sRNA sequence reads to the human genome using the short-read aligner Bowtie in the next step, and 69.3 million reads were mapped in all samples (Table S2). Then, we mapped these reads to the miRBase database; 7.26 million (51.98%), 7.90 million (54.84%), and 8.48 million (55.31%) total sRNA reads for the C1, C2, and C3 samples in the control group and 5.90 million (41.01%), 3.41 million (59.01%), and 1.81 million (33.77%) total sRNA reads for the I1, I2, and I3 samples in the ILAE type 1 group, respectively, were mapped to known miRNA. The classification and annotation of all small RNAs in each sample are summarized in Supplementary Fig. 3.

Comparative miRNA Expression in the ILAE Type 1 and Control Groups

MiRNA expression was assessed by normalizing them into TPM for each sample; Fig. 2a shows the TPM density distribution of each sample. A total of 1643 mature miRNAs and 1323 hairpin miRNAs were mapped with miRBase in the two groups of our samples. Of these miRNAs, 81 differentially expressed miRNAs were significantly dysregulated ($p < 0.05$) in the ILAE type 1 hippocampal samples compared with controls; 42 were upregulated and 39 were downregulated (Table S3). In the next step, the Benjamini–Hochberg method was used to control the FDR of the high-throughput sequence, and the adjusted p value was calculated. In this condition, 7 miRNAs were identified as having significantly different expression profiles between the ILAE type 1 and no-HS groups, including upregulation of hsa-miR-302a-5p, hsa-miR-1-3p, hsa-miR-302d-3p, hsa-miR-302a-3p, and hsa-miR-302b-3p and downregulation of hsa-miR-330-3p and hsa-miR-1307-3p. Hierarchical clustering and volcano plots illustrate these differentially expressed miRNAs (Fig. 2b, c). Among the different types of miRNA, 4 were upregulated and 1 was downregulated, with a fold change ≥ 2. The fold change expression values of the 7 identified miRNAs are listed in Table 2. Hsa-miR-302a-5p and hsa-miR-1307-3p were the most noticeably upregulated and downregulated miRNAs, respectively.

All 7 dysregulated miRNAs were validated by RT-PCR in 7 ILAE type 1 and 7 control samples. As observed, hsa-miR-302a-5p, hsa-miR-1-3p, hsa-miR-302d-3p,

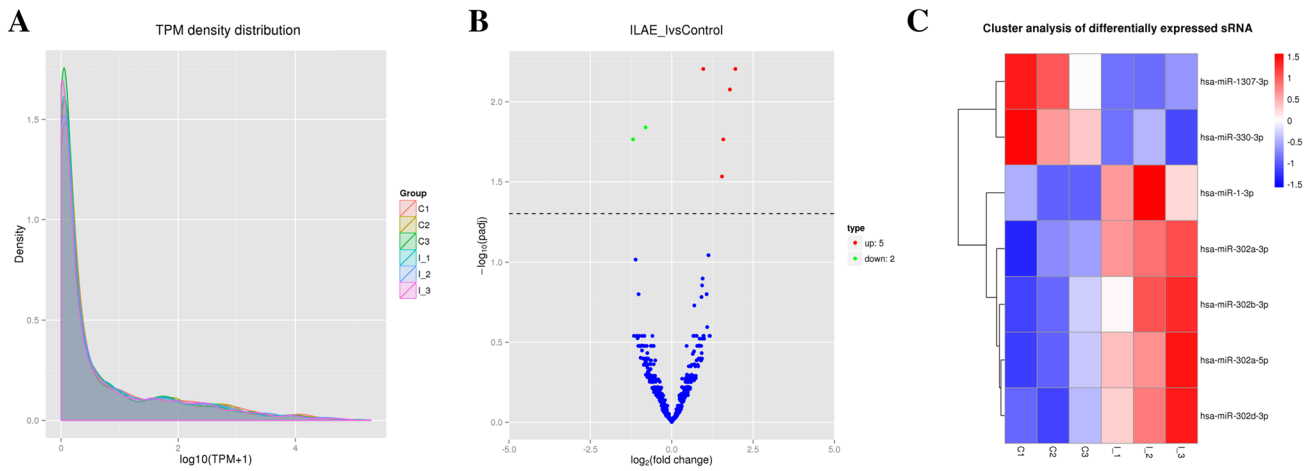

Fig. 2 Differentially expressed miRNAs between HS ILAE type 1 and no-HS type groups. **a** TPM density distribution of each sample. **b** The volcano plots illustrate the overall distribution of differentially expressed miRNAs. The abscissa represents the fold change of miRNA expression; these fold change values were transformed into a -log2 scale. The ordinate represents the statistical significance of the different miRNA expression; these adjusted *p* values were transformed into a -log10 scale. The scatter points in the figure represent the miRNAs: the blue dots represent the miRNAs with no significant difference in expression, the red dots represent the significantly increased miRNAs, and the green dots represent the significantly decreased miRNAs. **c** Heatmap representation of the expression levels of miRNAs in the ILAE type 1 (I1, I2, and I3) and no-HS (C1, C2, and C3) groups. Each row and column represents one miRNA and a sample tissue, respectively. The miRNA expression was determined by normalizing them into TPM and then transforming them into log10(TPM + 1) as the values in this heatmap. The red indicates upregulated expression, and the blue means downregulated expression

Table 2 Different expression miRNA between ILAE 1 and no-HS group

miRNA	Regulation	Log2 fold change	*p* value	Adjust *p* value
hsa-miR-302a-5p	up	1.9553	1.27E-05	0.0062402
hsa-miR-302d-3p	up	1.7869	4.16E-05	0.0083874
hsa-miR-302a-3p	up	1.5846	0.00015495	0.017199
hsa-miR-302b-3p	up	1.542	0.00033903	0.029302
hsa-miR-1-3p	up	0.96905	2.06E-05	0.0062402
hsa-miR-1307-3p	down	− 1.1896	0.00017057	0.017199
hsa-miR-330-3p	down	− 0.80377	9.56E-05	0.014457

hsa-miR-302a-3p, and hsa-miR-302b-3p were significantly upregulated in the ILAE type 1 group, while hsa-miR-330-3p and hsa-miR-1307-3p were downregulated (Fig. 3a–g). Thus, it is evident that the RNA-seq data were in accordance with the RT-PCR results.

Bioinformatics Analysis

We used the experimentally validated databases, miRDB and Targetscan, for miRNA target prediction, and 1545 target genes were predicted with 7 deregulated miRNAs (Fig. 3h). GO enrichment and KEGG pathway analysis were used for the bioinformatics analysis of dysregulated miRNAs. After adjusting the *p* value using the Benjamini–Hochberg procedure, a p value < 0.05 was considered a significantly enriched pathway.

The top 10 GO terms were significantly overrepresented in three basic categories: the cellular component, molecular function, and biological process (Fig. 4a–c). In the cellular component analysis, the targets were mostly enriched in intracellular ($n = 1261$), followed by intracellular part ($n = 1235$) and intracellular organelles ($n = 1110$). Nucleic acid binding ($n = 408$), followed by enzyme binding ($n = 224$) and transferase activity, as well as the transferring phosphorus-containing groups ($n = 131$), were the most enriched items based on each target in the molecular function analysis. The biological process analysis showed that the target genes were mainly located in the cellular macromolecule metabolic process ($n = 832$); further, there was regulation of the macromolecule metabolic process ($n = 639$) and regulation of the primary metabolic process ($n = 633$).

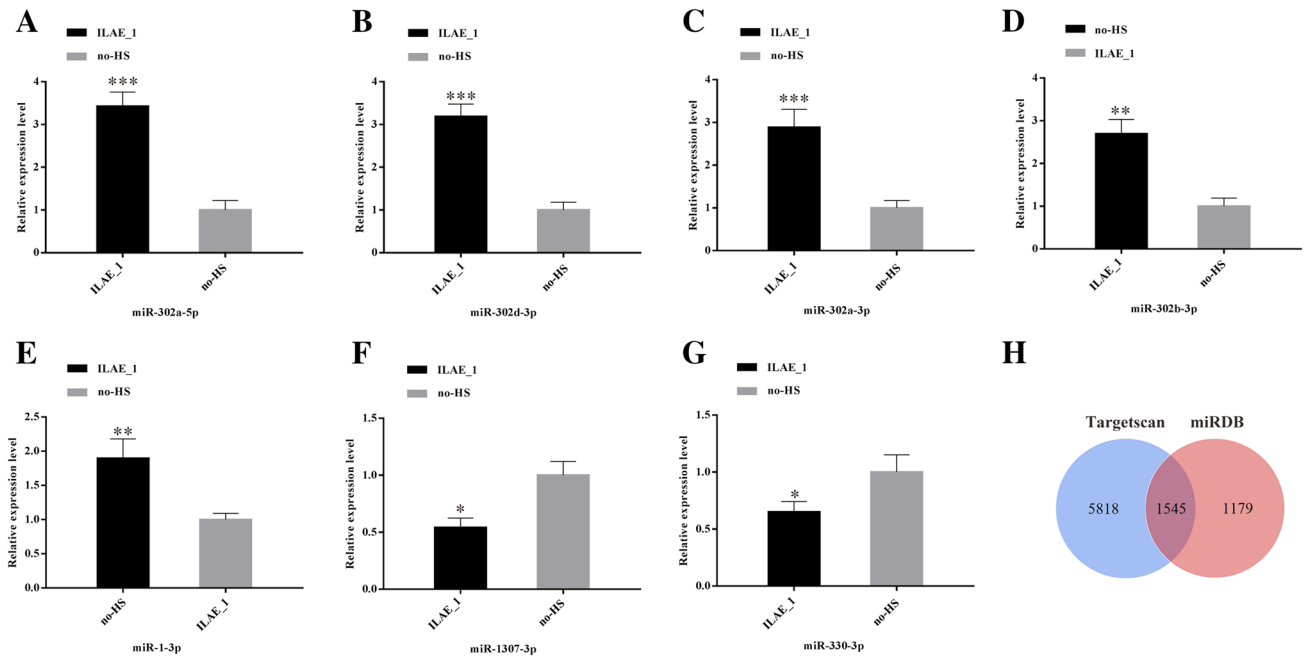

Fig. 3 Validation of differentially expressed miRNAs analyzed by real-time PCR and prediction of the targets of these miRNAs. **a**–**g** The expression levels of upregulated miRNAs (miR-302a-5p, miR-302d-3p, miR-302a-3p, miR-302b-3p, and miR-1-3p) and downregulated mRNAs (miR-1307-3p and miR-330-3p) were further validated by real-time PCR (2-ΔΔCt method). Statistically significant differences were determined using a Mann–Whitney test. Values are represented as the mean ± SEM ($n = 7$ for each group). $*p < 0.05$, $**p < 0.01$ $***p < 0.001$ compared with the no-HS group. **h** The MiRDB and Targetscan databases were used for dysregulated miRNA target prediction

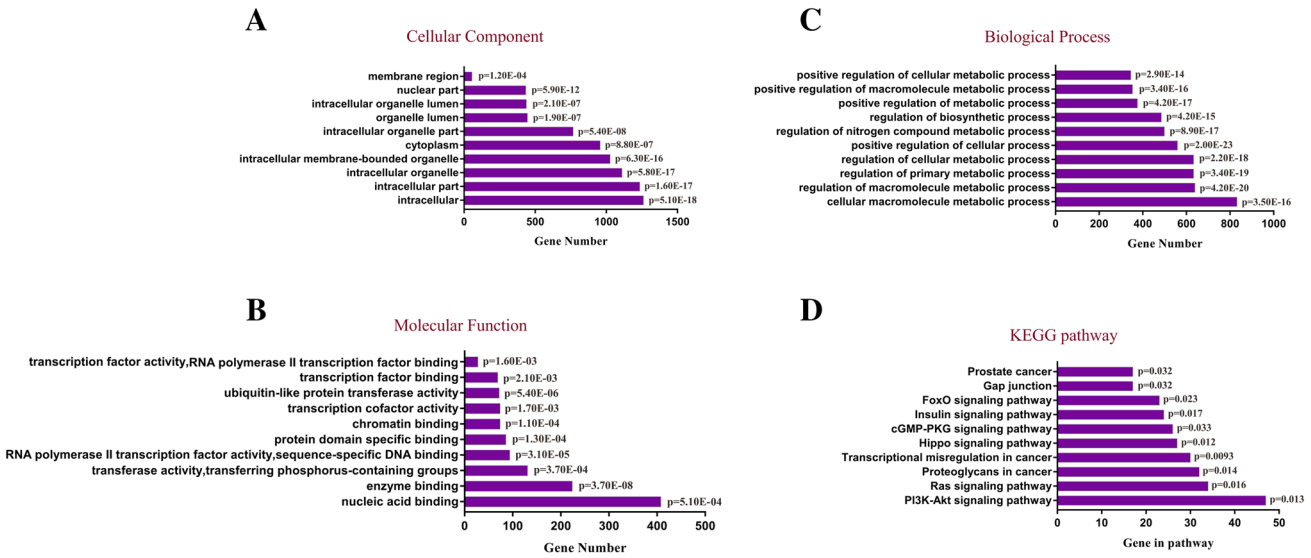

Fig. 4 Bioinformatics analysis of the differentially expressed miRNA targets. **a** Top 10 ranked terms in cellular component analysis. **b** Top 10 ranked terms in molecular function analysis. **c** Top 10 ranked terms in biological process analysis. **d** Top 10 ranked pathways in KEGG analysis. All *p* values underwent the Benjamini and Hochberg method for controlling FDR

The KEGG pathway analysis data, including pathway title, gene numbers, and the *p* values of the top 10 pathways, are shown in Fig. 4d, and the PI3K-Akt signaling pathway was enriched in most predicted target genes.

Discussion

In the current study, we provided the first evidence identifying the miRNA profile of the hippocampus in patients with epilepsy. The miRNA profile was differentially expressed, as determined by high-throughput sequencing in ILAE type 1 samples compared with the no-HS type (control) samples. Ultimately, we identified 7 significantly dysregulated miRNAs, some of which were upregulated (hsa-miR-302a-5p, hsa-miR-1-3p, hsa-miR-302d-3p, hsa-miR-302a-3p, and hsa-miR-302b-3p) and some of which were downregulated (hsa-miR-330-3p and hsa-miR-1307-3p), followed by further validation with RT-PCR.

Although previous studies have investigated miRNA expression in epilepsy patients and animal models, few studies have focused on their miRNA profile in the new HS ILAE subtype classification. Song et al. (Song et al. 2011) previously reported the altered miRNA expression profiles in the hippocampus in chronic lithium-pilocarpine-induced TLE rat models and identified that rno-let-7e and rno-miR-23a/b exhibited differential expression during epileptogenesis. Hu et al. (Hu et al. 2012) identified 24 deregulated miRNAs in a temporal lobe epilepsy model by miRNA microarray approach and found that rno-miR-34a played an important role in hippocampal neuronal apoptosis. Then, a genome-wide miRNA profiling study in human TLE was published. This research detected 165 miRNAs with up- or downregulated expression relative to those in the hippocampus of autopsy control patients and indicated that dysregulated miRNA correlated with immunomodulatory proteins (Kan et al. 2012). Another study of a whole-human hippocampal miRNome including 33 patients with TLE and 9 postmortem controls reported that 19 miRNAs were upregulated and one was downregulated. This study was the largest cohort of patients to be studied featuring HS in TLE thus far (Bencurova et al. 2017). Nevertheless, the results of this study, which included the differential expression of 7 miRNAs, did not correspond with the findings of the aforementioned studies. The reason might depend on sample selection and technical approach in different studies. In this study, the hippocampal samples were stored in liquid nitrogen immediately after surgical resection to prevent miRNA degradation. It is known that miRNA expression levels in epileptic rat models differ from those identified in epileptic patients (Kandratavicius et al. 2014). We focused on the epileptic subtype of brain tissue from patients with ILAE type 1 and no-HS type, which were proposed by ILAE, and found miRNA profile alterations. In addition, the NGS platform used in this research avoided the limitation of selected primers in predetermined profiling assays, such as microarrays.

HS ILAE type 1, the most common type, was characterized by severe neuronal loss in region CA1, while the no-HS type exhibited only reactive gliosis on pathological examination. However, disordered miRNAs could affect many pathways by regulating the entire network of genes involving gliosis, inflammation, and neuronal function (Henshall et al. 2016). The results of this study may have important implications for the pathological reasons underlying neuronal loss between ILAE type 1 and no-HS. The miR-302 cluster, which is a large miRNA family, exhibited upregulation of miR-302a, miR-302b, and miR-302d in this study; this phenomenon is best known for its role in the biological processes associated with antioxidative stress, antiapoptosis, and antiaging, which are accomplished through the Akt signaling pathway (Balzano et al. 2018; Li et al. 2016). Our results, which demonstrated enrichment of the PI3K-Akt signaling pathway, corresponded to the above suggestion. In Alzheimer's disease, animal models that are similar to the GFAP-positive epilepsy model in the hippocampus have shown overexpression of miR-302/367, which can reprogram reactive astrocytes to neurons in vivo (Ghasemi-Kasman et al. 2018). Additional research suggested that miR-302/367 could enhance neuronal regeneration following kainic acid-induced hippocampal neurodegeneration (Ghasemi-Kasman et al. 2017). All these results indicate that upregulation of the miR-302 family in HS ILAE type 1 may affect the regeneration of neurons compared with miR-302 family expression in no-HS type; however, this aspect of the study has not been reported until now. MiR-1, which was found to be upregulated in this research, is interrelated with brain development and neuronal function by targeting brain-derived neurotrophic factor (BDNF) (Varendi et al. 2014). Scant literature has explained the function of miR-1 in HS ILAE type 1. Some studies have suggested that the two downregulated miRNAs, namely, miR-330 and miR-1307, are primarily related to oxidative stress (Donato et al. 2018; Zhou et al. 2018). MiR-330 could aggravate oxidative stress and mitochondrial dysfunction in Alzheimer's disease by targeting VAV1 (Zhou et al. 2018). Notably, epileptogenesis and neuronal death were related to an imbalance between the antioxidant system and reactive oxygen species (ROS) generation caused by oxidative stress (Arena et al. 2018; Pansani et al. 2018). Another study found that PTEN-induced putative kinase 1 (PINK1) deficiency, which is a gene associated with Parkinson's disease, a neurodegenerative disease, reduces miR-330 expression and results in the regulation of GFAP expression (Choi et al. 2016), yet the mechanism of these miRNAs in ILAE type 1 has yet to be found.

Owing to strict filtering criteria, the sample size in our study was rather small, and the required miRNA dysregulation was validated in a large TLE ILAE type 1 sample. The more these subjects are investigated to determine the miRNA expression of TLE in HS [such as in Bencurova's

research ($n = 33$)], the more convincing the results are (Bencurova et al. 2017). One of the limitations of this study is the absence of patients with a pathology of HS ILAE types 2 and 3, which could have been compared with the no-HS control. As is known, types 2 and 3 TLE are uncommon, found in approximately 5–10% and 4–7.4% of all TLE surgical cases, respectively (Blümcke et al. 2013; Ghasemi-Kasman et al. 2017). However, our research group is currently collecting specimens of these two rare types for further research.

In summary, this study evaluated the miRNA profile of HS ILAE type 1 compared with the no-HS type via NGS and RT-PCR. We identified 7 dysregulated miRNAs, including upregulation of 5 miRNAs (miR-302a-5p, miR-302b-3p, miR-302d-3p, miR-302a-3p, and miR-1-3p) and downregulation of 2 miRNAs (miR-330-3p and miR-1307-3p), by analyzing two groups of patients ($n = 7$ in each group). Additionally, 1545 target genes were predicted using the miRDB and Targetscan databases, and these predicted genes demonstrated enrichment in the pathway associated with nucleic acid binding, intracellular and cellular macromolecular metabolic processes, and the PI3K-Akt signaling pathway. Although this research focused on patients with HS ILAE type 1, these results provide new insights into the neuronal loss pathology of type 1 TLE. Further research of aberrant miRNA expression in different ILAE subtypes might lead to an improved understanding of the pathogenesis of epilepsy.

Acknowledgements This work was supported by the National Nature Science Foundation of China (No. 81571646; No. 81601130; No. 81772678; No. 81572472; No. 81773161), Foundation of Heilongjiang Health and Family Planning Commission (2018375), Heilongjiang Provincial Postdoctoral Science Foundation (LBH-Z17144), and Postdoctoral Science Foundation of China (2018M631951).

Gene Bank The raw sequence data are submitted at GEO (GSE124507).

Author Contributions ZL: conception and design. CT and HW: performing the studies. HW, SY and ZH: tissue and immunohistochemistry. ZH, CT, ZJ and MN: RNA isolation, RNA-Seq and data analysis. CT and ZL: writing the paper. DL and MG: editing the paper. All authors read and approved the final manuscript.

Compliance with Ethical Standards

Conflict of interest The authors declare that they have no conflict of interest.

Ethical Approval All procedures performed in this study involving human participants were in accordance with the ethical standards of the First Clinical College Ethics Committee of Harbin Medical University and with the 1964 Helsinki declaration and its later amendments or comparable ethical standards. For minors/children less than 16 years enrolled in our study, we obtained written informed consent from the parents.

Informed Consent Informed consent was obtained from all individual participants included in this study.

References

Alsharafi WA, Xiao B, Abuhamed MM, Luo Z (2015) miRNAs: biological and clinical determinants in epilepsy. Front Mol Neurosci 8:59. https://doi.org/10.3389/fnmol.2015.00059

Arena A et al (2018) Oxidative stress and inflammation in a spectrum of epileptogenic cortical malformations: molecular insights into their interdependence. Brain Pathol. https://doi.org/10.1111/bpa.12661

Bagla S et al (2018) A distinct microRNA expression profile is associated with α[11C]-methyl-L-tryptophan (AMT) PET uptake in epileptogenic cortical tubers resected from patients with tuberous sclerosis complex. Neurobiol Dis 109:76–87. https://doi.org/10.1016/j.nbd.2017.10.004

Balzano F, Cruciani S, Basoli V, Santaniello S, Facchin F, Ventura C, Maioli M (2018) MiR200 and miR302: Two Big Families Influencing Stem Cell Behavior. Molecules 23. https://doi.org/10.3390/molecules23020282

Bencurova P et al (2017) MicroRNA and mesial temporal lobe epilepsy with hippocampal sclerosis: Whole miRNome profiling of human hippocampus. Epilepsia 58:1782–1793. https://doi.org/10.1111/epi.13870

Blümcke I et al (2007) A new clinico-pathological classification system for mesial temporal sclerosis. Acta Neuropathol 113:235–244. https://doi.org/10.1007/s00401-006-0187-0

Blümcke I et al (2013) International consensus classification of hippocampal sclerosis in temporal lobe epilepsy: a Task Force report from the ILAE Commission on Diagnostic Methods. Epilepsia 54:1315–1329. https://doi.org/10.1111/epi.12220

Choi I, Woo JH, Jou I, Joe EH (2016) PINK1 Deficiency Decreases Expression Levels of mir-326, mir-330, and mir-3099 during Brain Development and Neural Stem Cell Differentiation. Exp Neurobiol 25:14–23. https://doi.org/10.5607/en.2016.25.1.14

Dai J et al (2017) Comprehensive analysis of a microRNA expression profile in pediatric medulloblastoma. Mol Med Rep 15:4109–4115. https://doi.org/10.3892/mmr.2017.6490

Donato L, Bramanti P, Scimone C, Rinaldi C, D'Angelo R, Sidoti A (2018) miRNAexpression profile of retinal pigment epithelial cells under oxidative stress conditions. FEBS Open Bio 8:219–233. https://doi.org/10.1002/2211-5463.12360

Friedländer MR, Mackowiak SD, Li N, Chen W, Rajewsky N (2012) miRDeep2 accurately identifies known and hundreds of novel microRNA genes in seven animal clades. Nucleic Acids Res 40:37–52. https://doi.org/10.1093/nar/gkr688

Ghasemi-Kasman M, Baharvand H, Javan M (2017) Enhanced neurogenesis in degenerated hippocampi following pretreatment with miR-302/367 expressing lentiviral vector in mice. Biomed Pharmacother 96:1222–1229. https://doi.org/10.1016/j.biopha.2017.11.094

Ghasemi-Kasman M, Shojaei A, Gol M, Moghadamnia AA, Baharvand H, Javan M (2018) miR-302/367-induced neurons reduce behavioral impairment in an experimental model of Alzheimer's disease. Mol Cell Neurosci 86:50–57. https://doi.org/10.1016/j.mcn.2017.11.012

Henshall DC et al (2016) MicroRNAs in epilepsy: pathophysiology and clinical utility. Lancet Neurol 15:1368–1376. https://doi.org/10.1016/S1474-4422(16)30246-0

Hu K et al (2012) MicroRNA expression profile of the hippocampus in a rat model of temporal lobe epilepsy and miR-34a-targeted neuroprotection against hippocampal neurone cell apoptosis post-status epilepticus. BMC Neurosci 13:115. https://doi.org/10.1186/1471-2202-13-115

Kan AA et al (2012) Genome-wide microRNA profiling of human temporal lobe epilepsy identifies modulators of the immune

response. Cell Mol Life Sci 69:3127–3145. https://doi.org/10.1007/s00018-012-0992-7

Kandratavicius L et al (2014) Animal models of epilepsy: use and limitations. Neuropsychiatr Dis Treat 10:1693–1705. https://doi.org/10.2147/NDT.S50371

Kwan P et al (2010) Definition of drug resistant epilepsy: consensus proposal by the ad hoc Task Force of the ILAE Commission on Therapeutic Strategies. Epilepsia 51:1069–1077. https://doi.org/10.1111/j.1528-1167.2009.02397.x

Langmead B, Trapnell C, Pop M, Salzberg SL (2009) Ultrafast and memory-efficient alignment of short DNA sequences to the human genome. Genome Biol 10:R25. https://doi.org/10.1186/gb-2009-10-3-r25

Li HH et al (2016) miR-302 Attenuates Amyloid-β-Induced Neurotoxicity through Activation of Akt Signaling. J Alzheimers Dis 50:1083–1098. https://doi.org/10.3233/JAD-150741

McKiernan RC et al (2012) Reduced mature microRNA levels in association with dicer loss in human temporal lobe epilepsy with hippocampal sclerosis. PLoS ONE 7:e35921. https://doi.org/10.1371/journal.pone.0035921

Na M et al (2015) Long-term seizure outcome for international consensus classification of hippocampal sclerosis: a survival analysis. Seizure 25:141–146. https://doi.org/10.1016/j.seizure.2014.10.006

Pansani AP et al (2018) Long-term monotherapy treatment with vitamin E reduces oxidative stress, but not seizure frequency in rats submitted to the pilocarpine model of epilepsy. Epilepsy Behav 88:301–307. https://doi.org/10.1016/j.yebeh.2018.09.027

Roncon P et al (2015) MicroRNA profiles in hippocampal granule cells and plasma of rats with pilocarpine-induced epilepsy–comparison with human epileptic samples. Sci Rep 5:14143. https://doi.org/10.1038/srep14143

Song YJ et al (2011) Temporal lobe epilepsy induces differential expression of hippocampal miRNAs including let-7e and miR-23a/b. Brain Res 1387:134–140. https://doi.org/10.1016/j.brainres.2011.02.073

Sørensen SS, Nygaard AB, Nielsen MY, Jensen K, Christensen T (2014) miRNA expression profiles in cerebrospinal fluid and blood of patients with acute ischemic stroke. Transl Stroke Res 5:711–718. https://doi.org/10.1007/s12975-014-0364-8

Surges R et al (2016) Changes in serum miRNAs following generalized convulsive seizures in human mesial temporal lobe epilepsy. Biochem Biophys Res Commun 481:13–18. https://doi.org/10.1016/j.bbrc.2016.11.029

Tang C et al (2018) Targeting of microRNA-21-5p protects against seizure damage in a kainic acid-induced status epilepticus model via PTEN-mTOR. Epilepsy Res 144:34–42. https://doi.org/10.1016/j.eplepsyres.2018.05.001

Varendi K, Kumar A, Härma MA, Andressoo JO (2014) miR-1, miR-10b, miR-155, and miR-191 are novel regulators of BDNF. Cell Mol Life Sci 71:4443–4456. https://doi.org/10.1007/s00018-014-1628-x

Wang J et al (2015) Circulating microRNAs are promising novel biomarkers for drug-resistant epilepsy. Sci Rep 5:10201. https://doi.org/10.1038/srep10201

Zhou Y, Wang ZF, Li W, Hong H, Chen J, Tian Y, Liu ZY (2018) Protective effects of microRNA-330 on amyloid β-protein production, oxidative stress, and mitochondrial dysfunction in Alzheimer's disease by targeting VAV1 via the MAPK signaling pathway. J Cell Biochem 119:5437–5448. https://doi.org/10.1002/jcb.26700